

An Analytical Approach to Model Heterogeneous Recrystallization Kinetics Taking into Account the Natural Spatial Inhomogeneity of Deformation



HAIWEN LUO and SYBRAND VAN DER ZWAAG

The classical Johnson–Mehl–Avrami–Kolmogorov equation was modified to take into account the normal local strain distribution in deformed samples. This new approach is not only able to describe the influence of the local heterogeneity of recrystallization but also to produce an average apparent Avrami exponent to characterize the entire recrystallization process. In particular, it predicts that the apparent Avrami exponent should be within a narrow range of 1 to 2 and converges to 1 when the local strain varies greatly. Moreover, the apparent Avrami exponent is predicted to be insensitive to temperature and deformation conditions. These predictions are in excellent agreement with the experimental observations on static recrystallization after hot deformation in different steels and other metallic alloys.

DOI: 10.1007/s11661-015-3200-1

© The Minerals, Metals & Materials Society and ASM International 2015

I. INTRODUCTION

THE classical model for recrystallization kinetics is based on the concepts originally formulated by Johnson and Mehl,^[1] Avrami^[2] and Kolmogorov^[3] in the 1930s, and is now often called the JMAK model, in which a random distribution of nucleation sites is assumed, and then the fraction recrystallized X_V can be derived as

$$X_V = 1 - \exp(-kt^n). \quad [1]$$

This simple equation just includes two parameters: the rate parameter k and the Avrami exponent n . This exponent is usually determined by plotting the equation in a double logarithmic form and taking n to be the slope of a $\log(\ln(1/(1 - X_V)))$ vs $\log(t)$ plot, the latter also called JMAK plot. In practice, Eq. [1] is widely used as an empirical equation to analyze the measured kinetics of recrystallization and other reactions involving both nucleation and growth in steels and other alloys.^[4–9] In the classical JMAK theory, Eq. [1] is actually derived from the concept of extended volume, X_{vex} , *i.e.*, the fraction of material that would have recrystallized if the phantom nuclei were real.^[4] In the case of nucleation and growth kinetics in three dimensions are both time-dependent, the fraction recrystallized is:

$$X_V = 1 - \exp(-X_{\text{vex}}) \\ = 1 - \exp\left\{-f_s \left[\int_{\tau}^t G(t') dt'\right]^3 \int_0^{\tau} N(\tau') d\tau'\right\}, \quad [2]$$

where $G(t)$ and $N(t)$ are growth and nucleation rates, respectively; f_s is the geometrical factor, for an example, it is $4\pi/3$ for the spherical nuclei. By the comparison of Eqs. [1] and [2], it is known that the rate parameter k could be influenced by many factors, such as nucleation kinetics, growth kinetics, the geometrical shape of nuclei and dimensions of growth. In contrast, the Avrami exponent n only depends on the time dependence of nucleation and growth rate, rather than the rate itself; Therefore, n is a stable inherent physical parameter related to the underlying mechanisms of nucleation and growth. For the three-dimensional growth, Eq. [2] indicates that n is equal to 3 in the case of site saturation and a constant growth rate, 4 when both the rates of nucleation and growth are constant. However, such high values for n have only been measured for the recrystallization of the lightly deformed fine-grained metals; for example, Gordon^[10] studied the recrystallization of copper and obtained an Avrami exponent of approximately 4, identical to the value predicted by the JMAK model. Surprisingly, the majority of experimental studies on the recrystallization kinetics of steels and alloys yielded Avrami exponents lower than 2, without any microstructural evidence that the nuclei grew in fewer than 3 dimensions.^[4–9] Moreover, n is in many cases not a constant but decreases with proceeding recrystallization,^[4–16] which cannot be explained by Eq. [2] either. This is because the recrystallizing grains gradually grow into the regions with lower stored energy, leading to the immigration velocity of the recrystallizing grain boundaries decrease significantly with annealing time, as revealed by Vandermeer and Gordon on

HAIWEN LUO, Professor, is with the State Key Laboratory of Advanced Metallurgy, and also with the School of Metallurgical and Ecological Engineering, University of Science and Technology Beijing, 3 Xue Yuan Lu 30, Beijing 100083, P.R. China. Contact e-mail: luohaiwen@ustb.edu.cn SYBRAND VAN DER ZWAAG, Professor, is with the Faculty of Aerospace Engineering, Delft University of Technology, 2629 HS Delft, The Netherlands.

Manuscript submitted December 6, 2014.

Article published online November 5, 2015

aluminum^[11] Vandermeer and Rath on iron^[12] and Rath *et al.* on titanium.^[13] Such time-dependent growth rate G is generally described by

$$G = Ct^{-r}, \quad [3]$$

where C and r are both constants, and $r = 0.38$ for the recrystallization of iron as investigated by Vandermeer *et al.* This will change Eq. [2] to

$$X_V = 1 - \exp(-X_{Vex}) = 1 - \exp\left\{-\frac{f_s \cdot N_0 \cdot C^3}{(1-r)^3} \cdot t^{3(1-r)}\right\} \quad [4]$$

Therefore, in the case of recrystallization of iron with varying growth rate, the Avrami exponent is given by $n = 3(1-r) = 1.86$, which is a typical value of Avrami exponent and will be discussed later.

In order to explain the discrepancy between the simple model predictions and experimental recrystallization data, Humphreys *et al.*^[4] suggested that the heterogeneity of recrystallization should be responsible for the lower value of the Avrami exponent, which was confirmed more quantitatively by Chen and Van der Zwaag in a number of single grain-based simulations taking into account nucleus clustering and strain heterogeneity.^[14–16] Assuming a random nucleation, Song *et al.*^[17] and Liu *et al.*^[18] both studied the blocking effect arising from the anisotropic growth on the deviation from JMAK kinetics using Monte Carlo simulations combined with an analytical approach, and indeed found that anisotropic growth rate lead to a change of the Avrami exponent n , the latter even changes as a function of the transformed fraction. Juul Jensen and Godiksen^[19,20] have recently reviewed experimental results on recrystallization kinetics obtained by neutron and synchrotron X-ray methods and concluded that “every single grain has its own kinetics different from that of the other grains”, which is actually consistent with Humphrey’s suggestion. By assuming nuclei to grow as spheres with radii $r = At^{1-\alpha}$, the influence of different types of distributions of A and α on recrystallization kinetics, *i.e.*, the JMAK plots, was studied *via* geometric simulations. It was found that distributions in A and α may affect the microstructure and texture, but only a distribution of α could change the JMAK plots and the Avrami exponent.^[20] Later, Rios and Villa^[21] developed analytical expressions which were derived from the classical JMAK equation and able to take a distribution of growth velocities into account. With their analytical equations, they managed to produce the same results as Godiksen *et al.*

The original JMAK theory requires a strictly random distribution of nuclei whilst nuclei actually often develop at certain preferential sites in the deformed microstructure like triple junction, grain boundaries, and various types of deformation-induced bands and heterogeneities. For example, the clustered nucleation is often found during the recrystallization of Al alloys and steels. With computer simulations, Storm and Juul Jensen relatively recently studied the effects of an experimentally determined 3D distribution of clustered nuclei on

recrystallization kinetics.^[22] They found that the clustering of nucleation could indeed affect recrystallization kinetics. Next, Villa and Rios again presented a rigorous mathematical approach to extend the classical JMAK model to situations in which nuclei were not homogeneously located but located in clusters.^[23] They managed to derive an exact analytical solution by assuming that nucleation sites could follow a Matèrn cluster process and then produce quite similar results as Storm *et al.* Moreover, they^[24] used recent developments in stochastic geometry to revisit the classical JMAK theory and have developed a general analytical approach to situations in which nuclei are located in space in either homogeneous or inhomogeneous fashion. Alternatively, Rath and Pande^[25] have also extended the JMAK equation to situations where nuclei are not randomly distributed by incorporating the measured time dependence of the transformed volume, the area of migrating interfaces and the size of the largest nucleus from a systematic two-dimensional surface examination.

However, these modeling, either numerical or analytical, are only able to demonstrate the significant influence of spatial distributions of nuclei or individual growth velocities on recrystallization kinetics separately, although in reality both could have a distribution. Although these models make success in describing the variation of the transient Avrami exponent during recrystallization, they seldom produce a single value of mean Avrami exponent to represent the entire recrystallization so that it can be directly compared with a large volume of existing experimental measurements in references, in which the measurements are usually fitted by the simple JMAK equation with a single value of Avrami exponent. In addition, they also have difficulties in explaining some relevant experimental observations. For examples, the experimentally measured Avrami exponent is not only smaller than that predicted by the classical JMAK theory but also gradually decreases with the proceeding recrystallization.^[4,12] In particular, the recent numerical and analytical models^[20,21] predict that the slope of JMAK plot should increase with the proceeding recrystallization in the case of a distribution of growth rate (see Figure 4 in Reference 20 and Figure 1 in Reference 21). In the case of clustering of nucleation, it was predicted that the slope of JMAK plot should firstly decrease with time, and then turn to increase to a constant in the end of recrystallization, see Figure 3 in Reference 22 and Figure 4 Reference 23. Finally, these models seem not able to explain why the measured Avrami exponents often reach a value lower than 2 and become insensitive to temperature and deformation conditions in the case of recrystallization after hot deformation or during annealing. For examples, Lü *et al.*^[26] obtained the values of the Avrami exponent ranged from 0.70 to 1.37 for the recrystallization behavior of a 50 pct cold-rolled high-manganese TWIP steels during annealing. Luton *et al.*^[27] and Ruibal *et al.*^[28] found constant Avrami exponents smaller than 2 for a range of copper and low-alloy steels. Laasraoui and Jonas^[7] have found that, over a wide range of temperatures and strain rates, the Avrami exponent is less than 1 for static recrystallization in low

carbon steels containing various combinations of niobium, boron, and copper, and concluded that this exponent shows independence of temperature and deformation. Sellars^[29] also observed a similar independence of temperature and strain rate for C-Mn and stainless steels.

In this paper, we present a new analytical extension of JMAK equation taking into account local variations in deformation as present in real hot deformed samples. Using a different approach, we have derived an average Avrami exponent to characterize the entire recrystallization process from start to final stages so that it can be compared better with the reported values. This new extension is capable of explaining all relevant experimental observations.

II. THEORETIC MODEL FOR THE KINETICS OF HETEROGENEOUS RECRYSTALLIZATION

The present model starts from the idea that was originally put forward by Rollett *et al.*^[30] The material that is about to recrystallize can be divided into M classes, with the recrystallization kinetics in each class, labeled i , being described by the JMAK equation

$$X_v^i = 1 - \exp(-X_{vex}^i) = 1 - \exp(-k_i t^{n_i}) \quad i = 1 \dots M, \quad [5]$$

where X_{vex}^i is known as the extended volume in the classical JMAK theory, *i.e.*, the fraction of material which would have recrystallized if the phantom nuclei were real.^[4] In the case of nucleation and growth rates both varying with time, the extended volume in the i class is derived from Eq. [2] as:

$$X_{vex}^i = f_s \left[\int_{\tau}^t G^i(t') dt' \right]^3 \int_0^{\tau} N^i(\tau') d\tau'. \quad [6]$$

Obviously, k_i depends on the local driving force for that particular class, while n_i is determined by the time dependence of nucleation and growth rates during recrystallization. Since the recrystallization mechanism in each artificially divided class should be same, it can be reasonably expected that the time dependence of nucleation and growth rates in each class is equal or at least similar, *i.e.*, $n_i = n$. This assumption is also in line with the experimentally observed weak dependence of n on temperature and deformation conditions.^[7,29] Equations [5] and [6] can be solved only when the kinetics of nucleation and growth are known. Sessa *et al.*^[31] did prove that JMAK equation is correct provided the following two conditions are satisfied: one is that distribution of nuclei should be random; the other is that the extended volume must be computed by including the so-called phantom nuclei. Even if the nucleation in the bulk of recrystallizing material is not random, we can apply Eq. [1] in a class in which the nucleation is random. The class is not necessarily a continuous solid segment in the material, but just a mathematically required space that consists of several separated or

connected recrystallizing units, where the two requirements are satisfied. In this case, the overall recrystallized fraction can be deduced by integration

$$X_v = \int_{k_{min}}^{k_{max}} (1 - \exp(-kt^n)) f(k) dk, \quad [7]$$

where $f(k)$ is probability density of k_i distribution in the recrystallizing material.

To derive an analytical equation for the heterogeneous recrystallization kinetics, an expression for the distribution of the rate parameter k should be available. Our previous research^[32] assumed a uniform distribution of k for ease of computation, which is obviously not physically correct since the local strain distribution is seldom uniform in a hot deformed material. Godiksen *et al.* calculated the heterogeneous recrystallization kinetics assuming that the time dependence of the unimpinged radius of the individual grains is given by $r = At^{1-\alpha}$ and A has a distribution of uniform, log-normal, or $1/A$.^[20] Therefore, it seems necessary to derive an actual or at least approximate distribution of k from the reliable experimental or computational data.

In the case of static recrystallization after hot deformation, distribution of k should result from the heterogeneous plastic deformation; whilst the local strain distribution could be investigated by both experimental measurements and finite element simulation. For examples, Colas and Sellars measured the strain distribution during plane strain compression testing firstly on aluminum alloy^[33] and then austenitic stainless steel^[34] by a microgrid technique. Specimens were firstly split down the middle, and lines 0.508 mm apart were scribed by milling on the section plane. The coordinates of the mesh were photographed and measured with a traveling microscope before bolting the two halves together. After compression to a certain strain, each specimen was unbolted and the grid rephotographed. The most recent quantitative investigation of the deformation of the grid can be performed by some appropriate image analysis on a direct comparison of two SEM digital images taken at two different deformation states.^[35] With this approach, the equivalent strain contours over specimens at a certain nominal strain can be mapped. It was found that the local strain varied from 0.1 to 1.1, when nominal strain was between 0.46 and 0.73. Moreover, they found that the local strain variation in deformed materials was considerable and increased with strain and strain rate. Variation of local strain during deformation can also be calculated using Finite Element Methods. Shipway and Bhadeshia^[36] calculated the strain distribution for a cylindrical steel specimen (initial height 12 mm, radius 4 mm) compressed to a final length of 6 mm with an interfacial friction coefficient of 0.5. Their calculations showed that the longitudinal true strain was 0.69, but the effective strains were not greater than 0.1 in the dead zone, whereas in regions close to the center the effective strain is close to 1.0. Both studies revealed that the local strain distribution in the deformed metals shows the characteristics of a normal distribution: the strain close to the mean value is accommodated in a large fraction of the bulk. In particular, Smith *et al.*^[37]

were even able to directly give distribution of local strain in the sample after uniaxial compression using FEM, which is close to an approximate normal distribution. Since we are now still lack of enough knowledge on the accurate distribution of local strain after deformation, a simple assumption of normal distribution, which widely exists in nature, may be a reasonable for establishing the new model:

$$f^\varepsilon(\varepsilon) = \frac{1}{\sigma\sqrt{2\pi}} \cdot \exp\left[-\frac{(\varepsilon - \mu_\varepsilon)^2}{2\sigma_\varepsilon^2}\right], \quad [8]$$

where $f^\varepsilon(\varepsilon)$ is the probability density function of the local strain distribution, μ_ε and σ_ε are the mean value and the standard deviation, respectively. Mathematically, ε , as a scalar quantity like von Mises equivalent strain, can vary from the minus infinity to the plus infinity, but it is clearly not possible in a real material; instead, the local strain varies between the symmetrically lower and upper limit of $\varepsilon_{\min} = \mu_\varepsilon - N\sigma_\varepsilon$ and $\varepsilon_{\max} = \mu_\varepsilon + N\sigma_\varepsilon$ respectively. Physically, the lower limit could be approaching 0 as in the so-called dead zone; in order to be consistent with this physical constraint, the value of N employed in the simulation should be larger than 3 to make sure that $\mu_\varepsilon - N\sigma_\varepsilon \rightarrow 0$ and $\int_{\mu_\varepsilon - N\sigma_\varepsilon}^{\mu_\varepsilon + N\sigma_\varepsilon} f^\varepsilon(\varepsilon) d\varepsilon \rightarrow 1$. The preliminary simulation indicate that $N = 3$ has already given the integrated value of 99.74 pct.

Now we have to find relationship between the local strain ε and the rate parameter k . Equation [1] has another form as well documented in literature,

$$X_V = 1 - \exp\left[-0.693\left(\frac{t}{t_{0.5}}\right)^n\right], \quad [9]$$

where $t_{0.5}$ is the time for 50 pct accomplishment of recrystallization, it can be easily derived that k is equal to $0.69 \cdot t_{0.5}^{-n}$ from Eqs. [1] and [9]. While $t_{0.5}$ is a function of strain, strain rate ($\dot{\varepsilon}$), initial grain size (D_0) and temperature (T) in the case of static recrystallization and described by the following equation^[7-9]

$$t_{0.5} = C_0 D_0 \varepsilon^{-p} \dot{\varepsilon}^q \exp(-Q/RT), \quad [10]$$

where D_0 is the initial grain size of matrix before recrystallization; Q is activation energy for recrystallization and C_0 , p , and q all constants. Equation [10] can be inserted into $k = 0.69 \cdot t_{0.5}^{-n}$, leading to

$$k = C_1 \cdot \varepsilon^{p \cdot n}, \quad [11]$$

where C_1 is a constant with a value depending on the initial grain size, the deformation condition, and temperature. Thus, the rate parameter k shows an exponential dependence on the local strain. Now we can derive the cumulative distribution function of the rate parameter k in a recrystallizing material, $F^k(k)$ from the cumulative local strain distribution function, $F^\varepsilon(\varepsilon)$, as shown below:

$$\begin{aligned} F^k(k) &= P\{k_{\min} \leq x_k \leq k\} = P\{k_{\min} \leq C_1 \cdot \varepsilon^{p \cdot n} \leq k\} \\ &= P\left\{\left(\frac{k_{\min}}{C_1}\right)^{\frac{1}{p \cdot n}} \leq \varepsilon \leq \left(\frac{k}{C_1}\right)^{\frac{1}{p \cdot n}}\right\} \\ &= F^\varepsilon\left[\left(\frac{k}{C_1}\right)^{\frac{1}{p \cdot n}}\right] - F^\varepsilon\left[\left(\frac{k_{\min}}{C_1}\right)^{\frac{1}{p \cdot n}}\right]. \end{aligned} \quad [12]$$

ε follows a normal distribution between ε_{\min} and ε_{\max} ; moreover, $k_{\min} = C_1 \cdot \varepsilon_{\min}^{p \cdot n}$ and $\varepsilon_{\min} = \mu_\varepsilon - N\sigma_\varepsilon$; thus, Eq. [12] can be changed to

$$F^k(k) = F^\varepsilon\left[\left(\frac{k}{C_1}\right)^{\frac{1}{p \cdot n}}\right] - F^\varepsilon(\mu_\varepsilon - N \cdot \sigma_\varepsilon). \quad [13]$$

By differentiating Eq. [13], the distribution density of k , $f^k(k)$, can be derived from the distribution of local strain as follows:

$$\begin{aligned} f(k) &= \frac{d[F^k(k)]}{dk} = \frac{d\left[F^\varepsilon\left[\left(\frac{k}{C_1}\right)^{\frac{1}{p \cdot n}}\right]\right]}{d\varepsilon} \cdot \frac{d\varepsilon}{dk} \\ &\quad - \frac{d[F^\varepsilon(\mu_\varepsilon - N \cdot \sigma_\varepsilon)]}{d\varepsilon} \cdot \frac{d\varepsilon}{dk} \end{aligned} \quad [14]$$

This leads to

$$\begin{aligned} f^k(k) &= \frac{1}{p \cdot n} \cdot C_1^{-\frac{1}{p \cdot n}} \cdot k^{\frac{1}{p \cdot n} - 1} \cdot \frac{1}{\sqrt{2\pi} \cdot \sigma_\varepsilon} \\ &\quad \cdot \left\{ \exp\left\{\frac{\left[\left(\frac{k}{C_1}\right)^{\frac{1}{p \cdot n}} - \mu_\varepsilon\right]^2}{-2 \cdot \sigma_\varepsilon^2}\right\} - \exp\left(-\frac{N^2}{2}\right) \right\}. \end{aligned} \quad [15]$$

Equation [15] is then inserted into Eq. [7], leading to:

$$\begin{aligned} X_V &= \int_{C_1 \cdot (\mu_\varepsilon - N \cdot \sigma_\varepsilon)^{p \cdot n}}^{C_1 \cdot (\mu_\varepsilon + N \cdot \sigma_\varepsilon)^{p \cdot n}} \frac{1}{p \cdot n} \cdot C_1^{-\frac{1}{p \cdot n}} \cdot \frac{1}{\sqrt{2\pi} \cdot \sigma_\varepsilon} \cdot k^{\frac{1}{p \cdot n} - 1} \\ &\quad \cdot \left\{ \exp\left\{\frac{\left[\left(\frac{k}{C_1}\right)^{\frac{1}{p \cdot n}} - \mu_\varepsilon\right]^2}{-2 \cdot \sigma_\varepsilon^2}\right\} - \exp\left(-\frac{N^2}{2}\right) \right\} dk. \end{aligned} \quad [16]$$

Equation [16] indicates that the recrystallized fraction in the heterogeneously deformed bulk can be derived from a distribution of local strain, the latter being assumed as having a normal distribution. It, however, is still not enough to calculate a value of Avrami exponent that is directly comparable to experimental observations given in the literature, since most of the experimental data on recrystallization kinetics are analyzed by the

simple JMAK equation and just one value of the exponent is derived for the entire process. In order to produce fraction dependent value for n , *i.e.*, n_t , Eq. [16] has been differentiated yielding

$$n_t = \frac{d \ln(\ln(1/(1 - X_V)))}{d[\ln(t)]} \quad [17]$$

Next, we average the value of n_t between $X_V = 0.05$ and $X_V = 0.95$, similar to what is common practice in using the JMAK equation. Let the time for 5 pct recrystallization be t_1 and that for 95 pct recrystallization t_2 , then the average exponent for the entire process of recrystallization is given by

$$n_{av} = \frac{\int_{t_1}^{t_2} n_t dt}{t_2 - t_1}. \quad [18]$$

This average value, n_{av} , should be comparable to the values of Avrami exponent reported in the literature for relevant recrystallization experiments. When μ_e and σ_e in Eq. [16] for the local strain distribution are known, the recrystallized fraction can be calculated at the different values of C_1 , p and n . In particular, the local exponent n is chosen as 1.86, 3 or 4 in the case of site-saturated nucleation with decreasing growth rate in pure iron, constant growth rate with site-saturated nucleation and constant rates of both nucleation and growth respectively. P is between 3.55 and 3.81 for steels^[7] and chosen as 3.33 here. These values are employed in the present calculations. In addition, the preliminary calculations show $\int_{\mu_e - N\sigma_e}^{\mu_e + N\sigma_e} f^e(\epsilon) d\epsilon = 0.997$ and $\int_{C_1(\mu_e - N\sigma_e)^{p/n}}^{C_1(\mu_e + N\sigma_e)^{p/n}} f^k(k) dk = 0.971$ in the case of $N = 3$. They are very close to 1, indicating our approximate calculations have a satisfactory accuracy.

III. RESULTS AND DISCUSSION

A. A Decreasing Slope of JMAK Plots with the Proceeding Recrystallization

A typical normal distribution of local strain within the deformed bulk is shown in Figure 1(a), in which a narrow peak with a smaller standard deviation means a

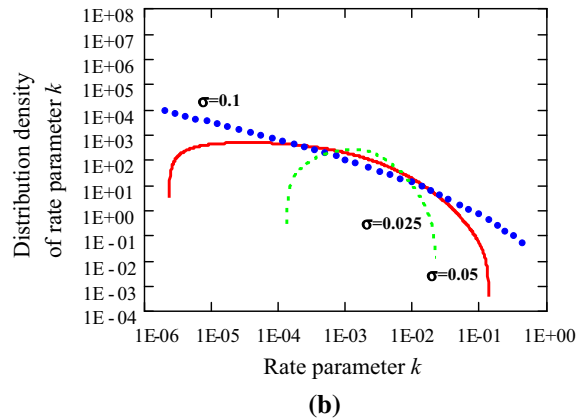
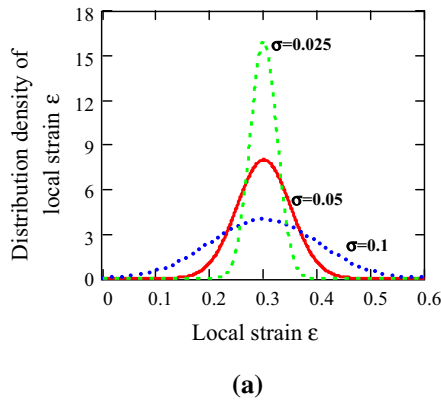


Fig. 1—The normal distribution of local strain (a) according to Eq. [8] and the derived distribution of rate parameter k (b) according to Eq. [14] using the values of $\mu = 0.3$, $C_1 = 400$, $p = 3.33$ and $n = 3$.

relatively uniform local strain distribution. In contrast, a slightly wider normal distribution of local strain leads to a very different curve for the distribution density of k as calculated by Eq. [15] and shown in Figure 1(b). It can be clearly seen that a larger standard deviation of local strain causes k to distribute over a much larger range.

Figure 2(a) shows the curves of recrystallized fraction *vs* time calculated by Eq. [16] at the given values of relevant parameters. Re-plotting the results of Figure 2(a) using double logarithm scales gives the typical JMAK plots whose slopes are the Avrami exponents, as shown in Figure 2(b). It can be seen that the JMAK plots have constant slopes at the beginning and then gradually decrease with the proceeding recrystallization, which successfully reproduces many experimental observations. Recrystallization will take place in a shorter time in the case of higher μ_e or C_1 or smaller σ_e , since all such conditions lead to a larger proportion of the bulk having high values of k_i , *i.e.*, fast recrystallization kinetics. It should be realized that an increasing n leads to a slowing down of the recrystallization kinetics (Curves 4 and 5 in Figure 2), which is different from the previous modeling results based on a uniform distribution of k_i .^[32] This is because the probability density of k actually decreases with increasing n according to Eq. [15]. By differentiating the JMAK plots according to Eq. [17], one may derive the instantaneous slope at each point of these curves, *i.e.*, the transient exponent n_t , which is shown in Figure 2(c). During recrystallization, n_t decreases with proceeding recrystallization. It decreases faster in the case of smaller μ_e , larger σ_e or higher n since they all result in either decreased driving force for recrystallization or smaller fraction of materials with high values of k ; whilst it is surprising to find that C_1 has no influence on n_t , an observation which is to be discussed later.

B. Dependence of the Average Exponent on the Local Strain Distribution

According to Eq. [18], the average Avrami exponents, n_{av} , can be derived by integrating n_t between 5 and 95 pct recrystallized fractions. Figure 3(a) shows the dependences of n_{av} on σ_e for given values of μ_e . The

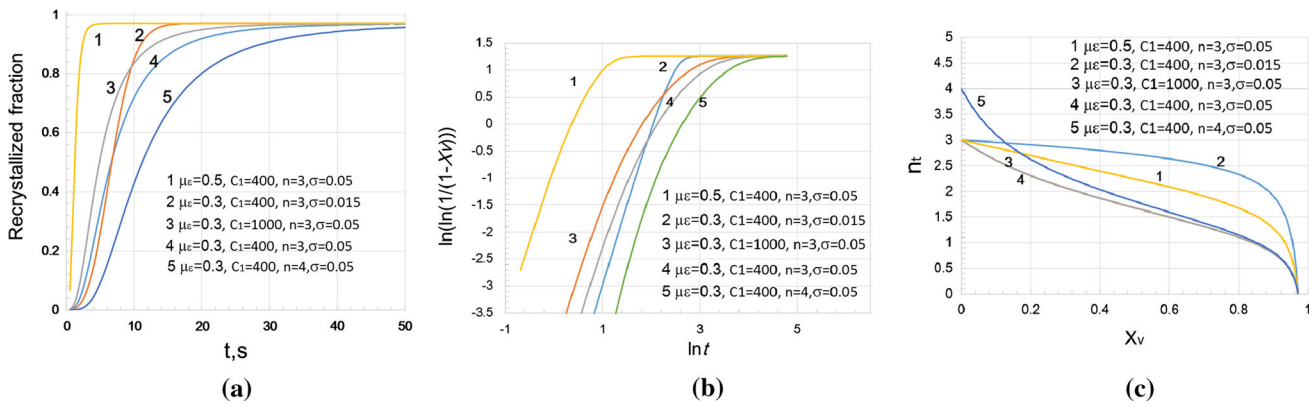


Fig. 2—Kinetics of heterogeneous recrystallization calculated with Eq. [16] at the given values of μ_e , σ_e , n , and C_1 (a) The curves of recrystallized fraction vs time. (b) The curves of $\ln(\ln(1/(1 - X_v)))$ vs $\ln(t)$, derived from (a); (c) The curves of instantaneous Avrami exponent of the recrystallizing material vs the recrystallized fraction, calculated by Eqs. [16] and [17].

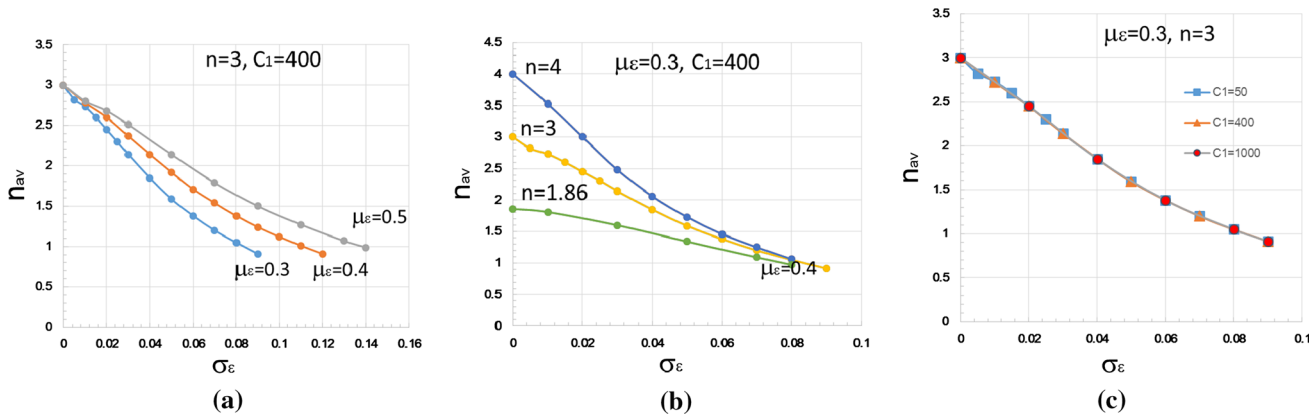


Fig. 3—Dependence of average Avrami exponent, n_{av} (derived by Eqs. [15] through [17]), on the standard deviation of local strain, σ_e , at the different values of (a) mean strain μ_e , (b) local exponent n and (c) constant C_1 .

curves of n_{av} vs σ_e are calculated until Eqs. [17] and [18] cannot produce convergent results in the case of $\mu_e - N\sigma_e$ approaching to 0. It is seen that both larger μ_e and smaller σ_e lead to higher exponent n_{av} . This is within expectation since larger μ_e means higher stored energy and smaller σ_e means larger proportion of bulk with the stored energy close to the mean value. In particular, n_{av} decreases faster with increasing σ_e when μ_e is smaller, *i.e.*, the variation of local strain appears to make a larger influence on n_{av} in the case of smaller nominal strain. When σ_e is large enough, n_{av} always decreases to about 1 irrespective of the value of μ_e . In other word, no matter how much nominal strain is applied, a heterogeneous enough distribution of local strain will result in a barely varying low Avrami exponent.

The local Avrami exponent, n , is an inherent physical parameter that reveals the mechanism of nucleation and growth. It may vary with the type or compositions of materials. However, a very different choice of n also makes little difference on the average exponent when the local strain variation is large enough, as shown in Figure 3(b). It can be seen that n_{av} always decreases to 1 in Figures 3(a) and (b), strongly suggesting that significant heterogeneous recrystallization kinetics will result

in the experimental Avrami exponent in a very narrow range. Since a varying n will not influence the average exponent remarkably in the case of heterogeneous enough distribution of local strain, $n_i \neq n$, *i.e.*, the assumption of $n_i = n$ in Eq. [5] is not valid, should not significantly change the results of n_{av} vs σ_e as shown in Figure 3b. In summary, a significant heterogeneity of recrystallization may mask the influence of other factors on the final average Avrami exponent.

Although C_1 is actually influenced by the initial grain size, deformation condition, and temperature according to Eqs. [10] and [11], Figure 3(c) shows that C_1 has no influence on n_{av} , at all, which is also consistent with independence of n_t on C_1 Figure 2(c). This is because that larger C_1 may accelerate recrystallization at the early stage but then decelerate it at the later stage, as shown in Figures 2(a) and (b). Hence the observed exponent should be insensitive to temperature and strain rate.

C. Range of the Observed and Actual Avrami Exponent

The relation between the actual Avrami exponent n for a very small and homogeneously deformed material volume and the average exponent n_{av} for real effectively

inhomogeneously deformed samples is shown in Figure 4. Also the values for n_{av} derived before for the case of a uniform distribution of k , are indicated. It is clear that the present approach predicts the narrowest range of the average exponent. The actual exponent, *i.e.*, the local exponent, only depends on the mechanism of nucleation and growth as mentioned before. The classical JMAK theory suggest that the actual Avrami exponent should be in the range of 1.86 to 4 for the different kinetics of nucleation and growth; in addition, the previous results based on the uniform distribution of k suggested a lower and narrower range of 0.75 to 2.2; while the present approach suggests the narrowest range between 1 and 2, converging to 1 when the variation in local strain is large enough, irrespective of the nucleation and growth kinetics, temperature and deformation condition, *etc.*

The above-derived average exponent n_{av} is characteristic for the entire recrystallization process so that it can be directly compared with the experimentally determined value of the Avrami exponent. Although the real value of σ_ϵ remains undefined, local strain may be reasonably expected to vary significantly for the usual deformation testing conditions on macroscopic samples. For an example, Colas and Sellars^[33–35] measured the strain distribution during plane strain compression testing on an austenitic stainless steel and found that the local strain could vary from 0.1 to 1.1 when nominal strain was between 0.46 and 0.73. Therefore, it could be a common phenomenon that hot deformation usually leads to a significant strain heterogeneity in the deformed bulk. In this case, the predication that the average exponent is between 1 and 2 and most often around 1 is quite consistent with experimental observations, because the measured exponents are seldom more

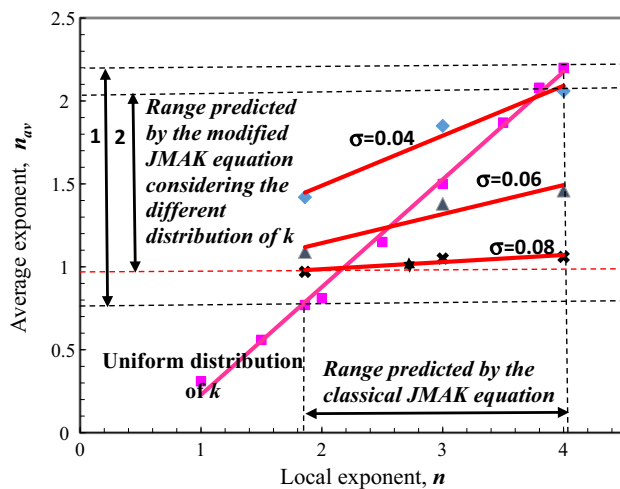


Fig. 4—Relationship of local exponent n , predicted by the classical JMAK equation, and the average exponent n_{av} , which is predicted by the present modified JMAK model to consider a normal distribution of local strain with the standard deviation of 0.04, 0.06, and 0.08, respectively. The arrows of '1' and '2' indicate the range of n_{av} when k distributes uniformly and according to Eq. [12] respectively. The former's data are from Ref. [31].

than 2, mostly in the range of 1 to 1.5. For examples, the experimentally observed exponent is 1 for C-Mn and Nb microalloying steels by Laasraoui and Jonas,^[7] 1.6 for a low carbon steel by Karjalainen *et al.*,^[5,6] in the range of 0.7 to 1.5 for 16 different steels as investigated by Medina and Quispe,^[9] 0.5 to 1.2 for very low carbon rolled steel by Michalak and Hibbard^[38] and 0.7 to 1.37 for high Mn TWIP steels by Lü *et al.*^[26] It is noted that the present approach predict that the lowest average exponent is 1; whilst the observed values could be lower than 1 sometimes. This is because the present model actually assumes that each part of the deformed bulk actually recrystallizes, *i.e.*, $k > 0$ in Eq. [5]. It, however, is not true in the case of low temperatures and small deformations, which may lead to some dead zones not recrystallizing at all. Consequently, the real average exponent could be even lower than the predicted values shown in Figures 3 and 4. In summary, Figure 4 explains why the observed Avrami exponents for the recrystallization of various alloys under very different test conditions necessarily are confined to a surprisingly narrow range.

It is noted that the present results demonstrate that the distribution of k influences the overall recrystallization kinetics greatly, which is different from the predictions by Godiksen and Juul Jensen *et al.*^[20] using 2D geometric computer simulations and those from Rios *et al.*^[21] using the analytical approach. They both have studied the recrystallization kinetics in the case that nuclei are site-saturated at the beginning and distribute randomly and grow with the radii $r = At^{1-\alpha}$ until impingement after assuming various distributions of A and α . They found that the distribution of A has no influence on the slope of JMAK plots but the distribution of α does, *i.e.*, k should not affect the Avrami exponent since the distribution of k is actually determined by that of A in this case. This difference results from the presumption of their models that the classical JMAK model can be actually applied in the entire deformed bulk because of the random distribution of nuclei; therefore, they have derived the expression of recrystallized fraction with the same form of Eq. [1], see Eq. [9] in Reference 21 so that variation of k does not influence the slope of JMAK plots at all. In contrast, we derived the overall recrystallization kinetics by averaging the kinetics of all recrystallizing classes using differentiation and integration as indicated by Eqs. [17] and [18]. Our model suggest that the distribution of k could influence the slope of JMAK plot even though every nucleus grows with the same value of n , *i.e.*, the same time dependence. Moreover, their models produce an upward curve in the JMAK plots whilst ours yield the downward curved plots consistent with experimental observation. In their very recent research on the recrystallization behavior of nanocrystalline copper,^[39] they have actually developed a quite similar model to deal with two-stage kinetics, in which two different values of k but a single value of n are used. By using this rather simple model, they have also shown that a distribution of k could influence on the Avrami exponent, leading to the measured values of n less than 1.

IV. CONCLUSIONS

Distribution density of the rate parameter k in JMAK equation is deduced from an assumed normal distribution of local strain values. Introduction of k distribution density of into the classical JMAK equation leads to a new analytical equation, by which the heterogeneous recrystallization kinetics can be calculated quantitatively. This new approach is not only able to describe influence of local strain heterogeneity on the overall recrystallization kinetics, but also to produce an average Avrami exponent to characterize the entire recrystallization process so that it can be directly compared with experimental measurements. In particular, it predicts that the apparent Avrami exponent, be within a narrow range of 1 to 2 converging to a value of 1 when the local strain varies greatly; moreover, this exponent is insensitive to temperature and deformation conditions. In addition, the model yields the JMAK plots having a constant slope at the beginning, and then the slope decreases gradually with proceeding recrystallization. These are in excellent agreement with the experimental observations on static recrystallization after hot deformation in different steels and other metallic alloys. Although the present model was developed for heterogeneous recrystallization kinetics, the expressions derived here may be applied to phase transformations involving nucleation and growth reactions.

ACKNOWLEDGMENTS

Haiwen Luo acknowledges the united financial support from National Natural Science Foundation of China and Bao Steel Group Co. Ltd. (No. U1460203) and International Science & Technology Cooperation Program of China (No. 2015DFG51950).

REFERENCES

1. W.A. Johnson and R.F. Mehl: *Trans. Am. Inst. Min. Metall. Eng.*, 1939, vol. 135, pp. 416–22.
2. M. Avrami: *J. Chem. Phys.*, 1939, vol. 71, pp. 1103–12.
3. A.E. Kolmogorov: *Bull. Acad. Sci. URSS*, 1937, vol. 1, pp. 355–59.
4. F.J. Humphreys and M. Hatherly: *Recrystallization and Related Annealing Phenomena*, 2nd ed., Elsevier Science Ltd., Oxford, 2004, pp. 232–48.
5. L.P. Karjalainen, T.A. Maccagno, and J.J. Jonas: *ISIJ Int.*, 1995, vol. 35, pp. 1523–31.
6. L.P. Karjalainen and J. Perttula: *ISIJ Int.*, 1996, vol. 36, pp. 729–36.
7. A. Laasoraoui and J.J. Jonas: *Metall. Trans. A*, 1991, vol. 22A, pp. 151–60.
8. W.P. Sun and E.B. Hawbolt: *ISIJ Int.*, 1997, vol. 37, pp. 1000–07.
9. S.F. Medina and A. Quispe: *ISIJ Int.*, 2001, vol. 41, pp. 774–81.
10. P. Gordon: *J. Met.*, 1955, vol. 201, pp. 1043–49.
11. R.A. Vandermeer and P. Gordon: *Trans. Metall. Soc. AIME*, 1959, vol. 215, pp. 577–88.
12. R.A. Vandermeer and R.A. Rath: *Metall. Mater. Trans. A*, 1989, vol. 20A, pp. 391–401.
13. B.B. Rath, R.J. Ledrerich, C.F. Yolton, and F.H. Froes: *Metall. Trans. A*, 1979, vol. 10A, pp. 1013–19.
14. S.P. Chen, I. Todd, and S. van der Zwaag: *Metall. Mater. Trans. A*, 2002, vol. 33A, pp. 529–37.
15. S.P. Chen and S. van der Zwaag: *Metall. Mater. Trans. A*, 2004, vol. 35A, pp. 741–49.
16. S.P. Chen and S. van der Zwaag: *Metall. Mater. Trans. A*, 2006, vol. 37A, pp. 2859–69.
17. S.J. Song, F. Liu, Y.H. Jiang, and H.F. Wang: *Acta Mater.*, 2011, vol. 59, pp. 3276–86.
18. F. Liu and G.C. Yang: *Acta Mater.*, 2007, vol. 55, pp. 1629–39.
19. D.J. Jensen and R.B. Godiksen: *Metall. Mater. Trans. A*, 2008, vol. 39A, pp. 3066–69.
20. R.B. Godiksen, S. Schimidta, and D.J. Jensen: *Scripta Mater.*, 2007, vol. 57, pp. 345–48.
21. P.R. Rios and E. Villa: *Scripta Mater.*, 2011, vol. 65, pp. 938–41.
22. S. Strom and D. Juul Jensen: *Scripta Mater.*, 2009, vol. 60, pp. 477–80.
23. E. Villa and P.R. Rios: *Acta Mater.*, 2009, vol. 57, pp. 3714–24.
24. P.R. Rios and E. Villa: *Acta Mater.*, 2009, vol. 57, pp. 1199–208.
25. B.B. Rath and C.S. Pande: *Acta Mater.*, 2011, vol. 59, pp. 7538–45.
26. Y.P. Lü, D.A. Molodov, and G. Gottstein: *Acta Mater.*, 2011, vol. 59, pp. 3229–43.
27. M.J. Luton, R.A. Petkovic, and J.J. Jonas: *Acta Metall.*, 1979, vol. 28, pp. 729–43.
28. E. Ruibal, J.J. Urcola, and M. Fuentes: *Z. Metall.*, 1985, vol. 76, pp. 568–76.
29. C.M. Sellars and G.J. Davies: *Hot Rolling and Forming Processes*, The Metal Society, London, 1980, pp. 3–15.
30. A.D. Rollett, D.J. Srolovitz, R.D. Doherty, and M.P. Anderson: *Acta Metall.*, 1989, vol. 37, pp. 627–39.
31. V. Sessa, M. Fanfoni, and M. Tomellini: *Phys. Rev. B*, 1996, vol. 54, pp. 836–41.
32. H.W. Luo, J. Sietsma, and S. van der Zwaag: *ISIJ Int.*, 2004, vol. 44, pp. 1931–36.
33. J.H. Beynon and C.M. Sellars: *J. Test. Eval.*, 1985, vol. 13, pp. 28–38.
34. R. Colas and C.M. Sellars: *J. Test. Eval.*, 1987, vol. 15, pp. 342–49.
35. C. Pinna, M. Bornert, J.H. Beynon, and C.M. Sellars: 39th Conference of Metallurgists, Ottawa, 2000.
36. P.H. Shipway and H.K.D.H. Bhadeshia: *Mater. Sci. Technol.*, 1995, vol. 11, pp. 1116–28.
37. A. Smith, A. Miroux, J. Sietsma, and S. van der Zwaag: *Steel Res. Int.*, 2006, vol. 77, pp. 595–602.
38. J.T. Michalak and W.R. Hibbard: *Trans. Am. Soc. Met.*, 1961, vol. 53, pp. 331–48.
39. F.X. Lin, Y.B. Zhang, N.R. Tao, W.G. Pantleon, and D. Juul Jensen: *Acta Mater.*, 2014, vol. 72, pp. 252–61.